



1-29-2022

## Determination of dissociation constants of protein ligands by thermal shift assay

Jaina A. Bhayani  
*Loyola University Chicago*

Miguel Ballicora  
*Loyola University Chicago, mballic@luc.edu*

Follow this and additional works at: [https://ecommons.luc.edu/chemistry\\_facpubs](https://ecommons.luc.edu/chemistry_facpubs)

 Part of the [Chemistry Commons](#)

### Recommended Citation

Bhayani, Jaina A. and Ballicora, Miguel. Determination of dissociation constants of protein ligands by thermal shift assay. *Biochemical and Biophysical Research Communications*, 590, : 1-6, 2022. Retrieved from Loyola eCommons, Chemistry: Faculty Publications and Other Works, <http://dx.doi.org/10.1016/j.bbrc.2021.12.041>

This Article is brought to you for free and open access by the Faculty Publications and Other Works by Department at Loyola eCommons. It has been accepted for inclusion in Chemistry: Faculty Publications and Other Works by an authorized administrator of Loyola eCommons. For more information, please contact [ecommons@luc.edu](mailto:ecommons@luc.edu).



This work is licensed under a [Creative Commons Attribution 4.0 International License](#).

© 2021 The Authors.



# Determination of dissociation constants of protein ligands by thermal shift assay



Jaina A. Bhayani, Miguel A. Ballicora\*

Department of Chemistry and Biochemistry, Loyola University Chicago, 1068 W. Sheridan Road, Chicago, IL, 60660, USA

## ARTICLE INFO

### Article history:

Received 10 December 2021

Accepted 14 December 2021

Available online 17 December 2021

### Keywords:

Protein–ligand affinity

Thermal shift assay

Dissociation constants

## ABSTRACT

The thermal shift assay (TSA) is a powerful tool used to detect molecular interactions between proteins and ligands. Using temperature as a physical denaturant and an extrinsic fluorescent dye, the TSA tracks protein unfolding. This method precisely determines the midpoint of the unfolding transition ( $T_m$ ), which can shift upon the addition of a ligand. Though experimental protocols have been well developed, the thermal shift assay data traditionally yielded qualitative results. Quantitative methods for  $K_d$  determination relied either on empirical and inaccurate usage of  $T_m$  or on isothermal approaches, which do not take full advantage of the melting point precision provided by the TSA. We present a new analysis method based on a model that relies on the equilibrium system between the native and molten globule state of the protein using the van't Hoff equation. We propose the  $K_d$  can be determined by plotting  $T_m$  values versus the logarithm of ligand concentrations and fitting the data to an equation we derived. After testing this procedure with the monomeric maltose-binding protein and an allosterically regulated homotetrameric enzyme (ADP-glucose pyrophosphorylase), we observed that binding results correlated very well with previously established parameters. We demonstrate how this method could potentially offer a broad applicability to a wide range of protein classes and the ability to detect both active and allosteric site binding compounds.

© 2021 The Authors. Published by Elsevier Inc. This is an open access article under the CC BY license (<http://creativecommons.org/licenses/by/4.0/>).

## 1. Introduction

The thermal shift assay (TSA) is a quick technique used to measure the thermal stability of a protein and detect protein–ligand binding [1]. It uses the qPCR instrument to monitor fluorescence and heat the protein at a controlled rate, exposing its hydrophobic core. Protein unfolding is tracked indirectly with dyes, like SYPRO Orange, that can bind to the nonpolar regions of a partially unfolded protein causing an increase in fluorescent emission [2–6].

Incrementally increasing the temperature shifts the protein equilibrium from a folded, native state ( $N$ ) towards a molten globule state ( $G$ ) (Fig. 1). The molten globule is a partially unfolded state of the protein resembling a native-like secondary structure with a loose tertiary structure [7–9]. The temperature at the point where the concentrations of  $N$  and  $G$  are equal is defined as the melting temperature of the protein [6,10,11]. A ligand ( $X$ ) that

preferentially binds to the native state will stabilize the protein and shift the equilibrium away from the molten globule. The degree of stabilization can be determined by comparing the melting temperature in the absence of ligand,  $T_{m0}$ , with that in the presence of ligand,  $T_m$ .

The thermal shift assay can be used with different protein types to detect compounds that can bind to the active and allosteric sites [4,12–15]. With the consumption of very little protein sample, as low as 25 nM, the thermal shift assay can screen a large library of ligands in less than an hour, allowing for high throughput analysis [1]. Furthermore, no structural knowledge is required to detect ligand binding in a TSA, a feature that makes this method ideal for proteins whose function is unknown [16].

Despite the benefits the TSA provides, this technique has been primarily used to qualitatively determine binding events [17]. Other methods, like isothermal titration calorimetry, can measure binding affinity and provide detailed thermodynamic parameters for the protein–ligand interaction [18]. However, it is low throughput and requires very large quantities of protein [19–22]. Past work has proposed several means of calculating dissociation constants ( $K_d$ ) from TSA data yet suffer from several drawbacks

Abbreviations: ADP-Glc PPase, ADP-Glucose Pyrophosphorylase; TSA, thermal shift assay; FBP, fructose 1,6-bisphosphate; MBP, maltose binding protein.

\* Corresponding author.

E-mail address: [mballic@luc.edu](mailto:mballic@luc.edu) (M.A. Ballicora).

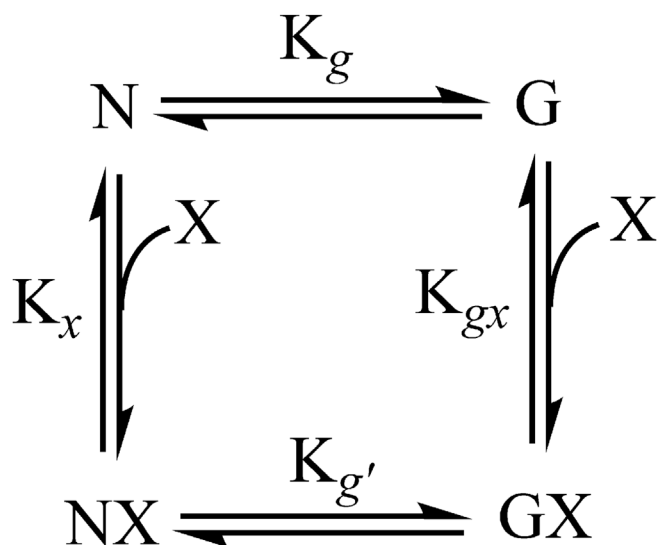


**Fig. 1.** Equilibrium diagram of the native and molten globule state in the presence of a ligand. The native state (N) of the protein is in equilibrium with the molten globule state (G) with an equilibrium constant  $K_g$ . The addition of ligand X produces NX and GX, and their respective dissociation constants,  $K_x$  and  $K_{gx}$ .

[2,23–26]. Recently, a robust method was developed to calculate  $K_d$  using the TSA, but it relies on an isothermal approach, where, at a given temperature, the changes in fluorescence are measured [26]. However, this does not utilize the greatest strength of the TSA, which is the precision in determining melting points [26]. Furthermore, precisely measuring isothermal changes in fluorescence heavily relies on the protein concentration of the sample [26].

Here, we present a new quantitative method for determining dissociation constants from TSA data. Our approach uses an equilibrium model derived from the van't Hoff equation and exploits the precise determinations of melting points using third degree differentiation. With this model, an equation that relates  $T_m$  vs. logarithm of the concentration of the ligand was derived and fit to the data to calculate the parameter  $K_d$ . The monomeric maltose binding protein (MBP) and a homotetrameric enzyme (*Escherichia coli* ADP-glucose pyrophosphorylase (ADP-Glc PPase)) were used as our sample protein models. Overall, the analysis method presented provides a rapid and straightforward way to determine dissociation constants between protein and ligands using the thermal shift assay.

## 2. Materials & methods

### 2.1. Biochemicals

Biochemicals used for the experiments were from Sigma-Aldrich (St. Louis, MO) and Thermo Fisher Scientific (Waltham, MA). All other chemicals were of the highest quality available.

### 2.2. MBP expression and purification

MBP, a common protein expression tag, was co-expressed and purified with human ornithine aminotransferase in a pMAL-c5X expression system. An N-terminal MBP tag was linked by a tobacco etch virus (TEV) cleavage sequence to the protein. Protein purification and production was performed as previously described [27]. TEV protease cleaved the fusion between the two proteins. MBP was then isolated by size exclusion chromatography using a

HiLoad Superdex-200PG column to apparent homogeneity as verified via SDS-PAGE. Fractions containing MBP were collected, concentrated to ~10 mg/ml, supplemented with 5% (vol/vol) glycerol, and stored at  $-80$  °C until use.

### 2.3. *E. coli* ADP-Glc PPase methods

Wild type and mutant ADP-Glc PPase were expressed and purified using the protocol previously described [28]. Activity was measured in the direction of ADP-glucose synthesis as previously published [28–30]. The parameter  $A_{0.5}$  (concentration of the activator needed to reach half of the maximum velocity) was determined by plotting and fitting to a Hill equation [29,31]. Site directed mutagenesis was performed as previously described [28] and the primers listed in Table S1 were used to make the mutants H46A, D385A, and E420A.

### 2.4. Thermal shift assays

Thermal shift assays were performed as described [28] using the QuantStudio 3 Real-Time PCR System™ (Thermo Fisher Scientific) and QuantStudio™ software. The final reaction volume was 20  $\mu$ l and contained 50 mM HEPES (pH 7.5), SYPRO Orange Dye (4X) and 25 nM purified protein, in the absence and presence of varying concentrations of ligand. A control with no protein was also performed for all the samples. A continuous temperature increase from 25.0 °C to 99.0 °C was scanned every 0.2 °C in a ramp increment of 0.1 °C per second. The third derivative of the fluorescence thermograms ( $d^3F/dT^3$ ) were obtained as follows. The averaged negative first derivative thermograms provided by the qPCR system were simultaneously smoothed and differentiated to the second degree in an Excel spreadsheet (Melting Point Calculator in Supplemental Materials) using a twenty-five-point Savitzky–Golay algorithm [32,33].

### 2.5. Data processing

The change of melting temperature versus the log of the ligand concentration was plotted and fit to the following equation:  $y = T_{m0} + A \log_{10}(1 + 10^x/K_d)$ , where  $y$  is the melting point of the protein ( $T_m$ ) at a given concentration of the ligand  $T_m$  and  $x$  is the logarithm of the ligand concentration. The parameter  $K_d$  is the dissociation constant of the ligand to the protein,  $T_{m0}$  is the melting point in absence of any ligand, and  $A$  is a parameter that encompasses the enthalpy of the protein melting, the gas constant  $R$ , and  $T_{m0}$ . Fitting was performed using the program Origin™ 9.1 with the Levenberg-Marquardt nonlinear least-squares algorithm. The errors of the parameters were obtained using that algorithm as well. All thermal shift assays were performed at least in triplicate with reproducibility of parameters within  $\pm 10\%$ .

## 3. Results and discussion

### 3.1. Temperature dependence of unfolding equilibrium

The protein heat denaturation can be described by temperature-induced changes to the equilibrium between the native and unfolded species (Fig. 1). To describe this phenomenon, we used a model based on the van't Hoff equation. Since the equilibrium constant ( $K_g$ ) between the native state and the molten globule is 1 at  $T_{m0}$ , and because the analysis is performed in a range of temperatures much smaller than the absolute temperatures (Supplemental Appendix), we approximate the van't Hoff equation to:

$$K_g = e^{\beta_g (T_m - T_{m0})} \quad (1)$$

Here,  $\beta_g = \frac{\Delta H_g}{RT_{m0}^2}$ , where  $\Delta H_g$  is defined as the enthalpy change in the conversion from  $N$  to  $G$ . Eq. (1) is identical to the “Boltzmann-like” empiric equation previously used to fit temperature-induced denaturation data, which supports the validity of our approximation [26].

### 3.2. Effect of one ligand binding site on protein melting points

To understand the melting point shift caused by the presence of a ligand, the equilibrium between the different protein forms and the ligand needs to be analyzed (Fig. 1). In presence of ligand  $X$ , the fraction ( $\varphi$ ) of protein that exists as molten globule is:

$$\varphi = \frac{\sum G}{\sum G + \sum N} = \frac{[G] + [GX]}{[G] + [GX] + [N] + [NX]} \quad (2)$$

Considering all the equilibrium constants ( $K_g$ ,  $K_{gx}$ , and  $K_x$ ) and that  $\varphi = 0.5$  at  $T_m$ , we use Eqs. (1) and (2) to obtain:

$$T_m = T_{m0} + \frac{1}{\beta_g} \ln \left( \frac{1 + [X]/K_x}{1 + [X]/K_{gx}} \right) \quad (3)$$

We can assume that in most cases the ligand has a much lower affinity for the molten globule state [34]. Then, the ranges at which the ligand  $X$  are analyzed will be much smaller than the constant  $K_{gx}$ . Therefore, Eq. (3) is further simplified.

$$T_m = T_{m0} + \frac{1}{\beta_g} \ln \left( 1 + \frac{[X]}{K_x} \right) \quad (4)$$

### 3.3. Graphical extrapolation of ligand affinity

It is implicitly assumed in Eq. (4) that  $K_x$  does not change significantly in the range of the temperatures assayed. This means that  $K_x$  is equal to  $K_{x0}$ , which is defined as the dissociation constant at  $T_{m0}$ . To account for temperature variations of  $K_x$  using a similar approximation of the van't Hoff equation and replacing into Eq. (4) (Supplemental Appendix), we get the following:

$$T_m = T_{m0} + \frac{1}{\beta_g} \ln \left( 1 + \frac{[X]}{K_{x0} e^{\beta_x (T_m - T_{m0})}} \right) \quad (5)$$

Here,  $\beta_x = \frac{\Delta H_x}{RT_{m0}^2}$ , which is a constant that takes into account the enthalpy change of the ligand dissociation process ( $\Delta H_x$ ). Nevertheless, this equation is inconvenient for fitting because  $T_m$  cannot be resolved as a dependent variable. However, at high concentrations of  $X$ , Eq. (5) becomes:

$$(\beta_g + \beta_x) (T_m - T_{m0}) = \ln[X] - \ln K_{x0} \quad (6)$$

The plot of  $T_m - T_{m0}$  vs  $\ln[X]$  is a straight-line where the x-intercept is  $\ln K_{x0}$ . This indicates that this extrapolation finds the dissociation constant of the ligand at  $T_{m0}$ . Even if the temperature dependence of  $K_x$  is significant, the slope of the straight line at high concentrations of  $X$  would be affected ( $\frac{1}{\beta_g + \beta_x}$  rather than  $\frac{1}{\beta_g}$ ), but not the x-intercept.

### 3.4. Proteins with multiple binding sites

In cases where a protein has more than one ligand-binding site,

a model that relates melting points and ligand concentration could be too complex and the number of parameters involved in an equation may make the solution impractical. For that reason, we chose to describe the ligand binding empirically with the Hill equation [35] (Supplemental Appendix).

$$T_m = T_{m0} + \frac{1}{\beta_g} \ln \left( 1 + \frac{[X]^n}{K_{0.5}^n} \right) \quad (7)$$

Here,  $K_{0.5}$  is the amount of ligand needed to reach half saturation and  $n$  is a parameter that describes their cooperativity. At high concentrations of  $X$ , this curve will also be a straight-line where the x-intercept is  $\ln K_{0.5}$ .

### 3.5. Calculation of dissociation constants

Using these derived equations, there are two ways to calculate  $K_x$ . One of them is by the method of extrapolation (Eq. (6)), and the other is by fitting the data of  $T_m$  vs  $\log[X]$  (or alternatively  $\ln[X]$ ) with a non-linear regression software (Eq. (4)). The first one provides a clear graphical understanding of how to interpret the data with a clear definition of the temperature at which  $K_x$  was obtained ( $K_{x0}$  at  $T_{m0}$ ). The graphical procedure to calculate  $K_{0.5}$  if the system contains more than one binding site is identical to the graphical procedure to calculate  $K_x$  for a protein with only one site.

Fitting the data is more precise and it should be the method of choice. Based on Eq. (4), the  $K_x$  obtained seems to be an average of the dissociation constant at the range of the  $T_m$  examined. In practice, the value obtained is within the experimental error of  $K_{x0}$ . This is because the most dominant part of the curve is the one at high concentrations of ligand. According to Eq. (6), this part determines the  $K_{x0}$  value. When we fit simulated data points based on Eq. (5) with Eq. (4), we obtain values that are within 10% error of  $K_{x0}$  (not shown). To calculate  $K_{0.5}$  if the system contains more than one binding site, Eq. (7) could be used to fit the data.

### 3.6. Experimental determination of MBP dissociation constants

To test the above theory, we performed thermal shift assays with MBP and compared the results with previously published data. Using the TSA, MBP had a  $T_m$  of approximately 48.6 °C in the absence of ligands, which was similar to previously reported melting temperatures [26]. Upon addition of maltose or maltotriose, MBP was stabilized shifting the thermograms to higher temperatures (Fig. S1). Increases in melting temperatures became apparent after a certain threshold was reached in the plot versus log of ligand concentration (Fig. 2). With our fitting method, the  $K_d$  of maltose and maltotriose was 698 ± 124 nM and 139 ± 22 nM, respectively. These  $K_d$  values correlate with previously published values, which range from 1000 to 1490 nM for maltose and 160–380 nM for maltotriose (Table 1) [36,37].

### 3.7. Experimental determination of ADP-Glc PPase dissociation constants

The method in this work hinges on the ability of a ligand to stabilize a protein, which was tested above with a simple monomeric protein. We investigated if the same rationale applied to different quaternary structures. Therefore, we used the tetrameric protein ADP-Glc PPase from *E. coli*. This enzyme uses ATP and Glc1P as substrates, with  $Mg^{2+}$  as a cofactor and fructose 1,6-bisphosphate (FBP) and AMP as allosteric regulators, to produce ADP-Glc and PPI [38]. Previously, equilibrium dialysis was used to determine  $K_d$  values for ADP-Glc PPase with its substrates and allosteric regulators (Table S2) [39]. These experiments required

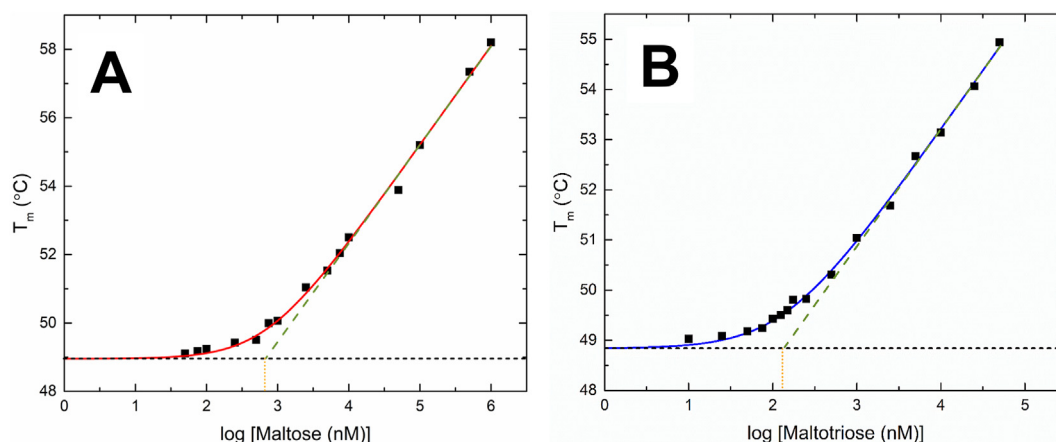


**Fig. 2. Maltose and maltotriose binding to MBP, as probed via TSA.** Data were collected in the presence of increasing maltose and maltotriose concentrations. The solid lines are the results of fitting the data with Eq. (4). The dashed green lines represent the linear extrapolation of the curve at higher concentrations and the black dashed lines represent the  $T_m$  in absence of ligands. These two lines intersect at the log of the  $K_d$  value (vertical orange dots). (For interpretation of the references to colour in this figure legend, the reader is referred to the Web version of this article.)

**Table 1**

Comparison of binding constants for MBP ligands with different methods.

Method	Maltose ( $K_d$ ) (nM)	Maltotriose ( $K_d$ ) (nM)	Protein Concentration (nM)	Reference
Fluorescence Quenching	1000	160	50–100	[36]
Equilibrium Dialysis	1490	380	320	[37]
Thermal Shift Assay	$698 \pm 124$	$139 \pm 22$	25	This work

high concentrations of enzyme (40  $\mu\text{M}$ ) while only being able to detect binding constants in the low micromolar range. To measure dissociation constants of higher values, higher concentrations of protein are needed. For the conditions used in those experiments, the authors reported that the detection of  $K_d$  values were limited to less than  $\sim 200 \mu\text{M}$ . Therefore, they were unable to detect the binding of the substrate Glc1P. Here, using only 25 nM of protein we were able to detect Glc1P binding in the absence of ATP with a  $K_d$  of 1640  $\mu\text{M}$ . Considering this result and that the  $K_d$  (in presence of CrATP) and  $K_m$  (in presence of ATP) for Glc1P are between 10 and 20  $\mu\text{M}$ , we can conclude that Glc1P will bind three orders of magnitude worse in absence of ATP, rather than not binding at all [39].

The TSA combined with our data analysis present a distinct advantage because it needs very little enzyme and has a broader range of detection for dissociation constants. With our method, range at which  $K_d$  can be measured does not depend on the protein concentration. In this case, the ability to detect the binding of Glc1P to the enzyme in the absence of ATP also offers insight into the kinetic mechanism. It was previously suggested that the kinetic mechanism for ADP-Glc PPase was ordered with ATP binding first and Glc1P second [40]. However, our TSA results suggest that the binding of substrates is not ordered but random and highly cooperative. With such high cooperativity, a random mechanism is kinetically indistinguishable from a true ordered mechanism [41]. Being able to detect binding with higher dissociation constants, like the ones shown here, could provide more information in understanding enzyme mechanisms.

### 3.8. Experimental determination of ADP-Glc PPase dissociation constants after mutagenesis

The method presented in this work can also be very useful to detect changes in ligand affinity after protein mutagenesis. To

illustrate this, we correlated changes in binding affinity with  $A_{0.5}$  after site-directed mutagenesis was performed on the allosteric binding site of the *E. coli* ADP-Glc PPase. Previously, charged residues surrounding the activator (FBP) binding site were replaced with alanine [28]. We chose FBP because allosteric effectors bind in rapid equilibrium, which means that binding affinity should correlate with kinetic parameters [41]. That is not necessarily the case with  $K_d$  and  $K_m$  of substrates participating in steady state reactions [41]. The results obtained by kinetic studies of FBP activation were comparable to the  $K_{0.5}$  obtained via the TSA method (Table 2). When the ratios between the  $K_{0.5}$  of the mutants over the  $K_{0.5}$  of the WT were compared to the ratios between the  $A_{0.5}$  of the mutants over the  $A_{0.5}$  of the WT, both sets of parameters changed similarly (Table 2). The  $R$  correlation coefficient between  $K_{0.5}$  and  $A_{0.5}$  was 0.994 (Fig. S2). This indicates that the procedure described here can quantify binding changes effectively after a site has been disrupted. The values for  $K_{0.5}$  were slightly but consistently higher

**Table 2**

Correlation between kinetic and binding parameters of the *E. coli* ADP-glucose pyrophosphorylase activator FBP.

Enzyme <sup>a</sup>	FBP			
	$K_{0.5}$ (mM)	$A_{0.5}$ (mM)	$K_{0.5}/K_{0.5(\text{WT})}$	$A_{0.5}/A_{0.5(\text{WT})}$
WT	$0.06 \pm 0.010$	$0.027 \pm 0.009^b$	1	1
R419A	$0.066 \pm 0.014$	$0.036 \pm 0.011^b$	1.1	1.3
R353A	$0.045 \pm 0.014$	$0.040 \pm 0.010^b$	0.75	1.5
E420A	$0.080 \pm 0.014$	$0.045 \pm 0.010^b$	1.3	1.7
R130A	$0.15 \pm 0.050$	$0.067 \pm 0.012$	2.5	2.5
D385A	$0.27 \pm 0.05$	$0.19 \pm 0.09$	4.5	7.0
R423A	$0.46 \pm 0.18$	$0.32 \pm 0.05^b$	7.7	11.9
H46A	$1.00 \pm 0.49$	$0.47 \pm 0.15$	16.7	17.4
R386A	$2.06 \pm 0.43$	$1.00 \pm 0.13^b$	34.3	37.0

<sup>a</sup> Kinetic and thermal shift assays were performed as described in Materials and Methods.

<sup>b</sup>  $A_{0.5}$  values were obtained from literature as described in Materials and Methods.

than the  $A_{0.5}$  values. That is expected because  $K_{0.5}$  values were determined around 53 °C ( $T_m$  of the protein) whereas the  $A_{0.5}$  were assayed at 37 °C. However, the relative influence of the mutations on  $A_{0.5}$  and  $K_{0.5}$  were nearly identical (Table 2).

#### 4. Conclusions

The TSA is a reliable, high throughput technique that gives an easy qualitative determination of ligand binding. Here, we show a new way to analyze thermograms to quantify dissociation constants with a simple equation (Eq. (4)). These dissociation constants are determined at the melting point the protein with high precision with very little protein. This is a rapid method to determine binding affinities, which will make it well suited for drug development projects and protein engineering studies.

#### Funding

This work was supported by a grant from the NSF(MCB 1616851 to MAB).

#### Declaration of competing interest

The authors declare they have no known competing financial interests or relationships that could have appeared to influence the work reported in this paper.

#### Appendix A. Supplementary data

Supplementary data to this article can be found online at <https://doi.org/10.1016/j.bbrc.2021.12.041>.

#### References

- [1] K. Gao, R. Oerlemans, M.R. Groves, Theory and applications of differential scanning fluorimetry in early-stage drug discovery, *Biophys. Rev.* 12 (2020) 85–104, <https://doi.org/10.1007/s12551-020-00619-2>.
- [2] M.C. Lo, A. Aulabaugh, G. Jin, R. Cowling, J. Bard, M. Malamas, G. Ellestad, Evaluation of fluorescence-based thermal shift assays for hit identification in drug discovery, *Anal. Biochem.* 332 (2004) 153–159, <https://doi.org/10.1016/j.ab.2004.04.031>.
- [3] F.H. Niesen, H. Berglund, M. Vedadi, The use of differential scanning fluorimetry to detect ligand interactions that promote protein stability, *Nat. Protoc.* 2 (2007) 2212–2221, <https://doi.org/10.1038/nprot.2007.321>.
- [4] G.A. Holdgate, M. Anderson, F. Edfeldt, S. Geschwindner, Affinity-based, biophysical methods to detect and analyze ligand binding to recombinant proteins: matching high information content with high throughput, *J. Struct. Biol.* 172 (2010) 142–157, <https://doi.org/10.1016/j.jsb.2010.06.024>.
- [5] O. Fedorov, F.H. Niesen, S. Knapp, Kinase inhibitor selectivity profiling using differential scanning fluorimetry, *Methods Mol. Biol.* 795 (2012) 109–118, [https://doi.org/10.1007/978-1-61779-337-0\\_7](https://doi.org/10.1007/978-1-61779-337-0_7).
- [6] G. Senisterra, I. Chau, M. Vedadi, Thermal denaturation assays in chemical biology, *Assay Drug Dev. Technol.* 10 (2012) 128–136, <https://doi.org/10.1089/adt.2011.0390>.
- [7] M. Ohgushi, A. Wada, 'Molten-globule state': a compact form of globular proteins with mobile side-chains, *FEBS Lett.* 164 (1983) 21–24, [https://doi.org/10.1016/0014-5793\(83\)80010-6](https://doi.org/10.1016/0014-5793(83)80010-6).
- [8] O.B. Pitsyn, R.H. Pain, G.V. Semisotnov, E. Zerovnik, O.I. Razgulyaev, Evidence for a molten globule state as a general intermediate in protein folding, *FEBS Lett.* 262 (1990) 20–24, [https://doi.org/10.1016/0014-5793\(90\)80143-7](https://doi.org/10.1016/0014-5793(90)80143-7).
- [9] M. Oliveberg, A.R. Fersht, Thermodynamics of transient conformations in the folding pathway of barnase: reorganization of the folding intermediate at low pH, *Biochemistry* 35 (1996) 2738–2749, <https://doi.org/10.1021/bi950967t>.
- [10] A.F. Rudolf, T. Skovgaard, S. Knapp, L.J. Jensen, J. Berthelsen, A comparison of protein kinases inhibitor screening methods using both enzymatic activity and binding affinity determination, *PLoS One* 9 (2014), e98800, <https://doi.org/10.1371/journal.pone.0098800>.
- [11] J. Hall, A simple model for determining affinity from irreversible thermal shifts, *Protein Sci.* 28 (2019) 1880–1887, <https://doi.org/10.1002/pro.3701>.
- [12] A.L. Klingner, D.F. McComsey, V. Smith-Swintosky, R.P. Shank, B.E. Maryanoff, Inhibition of carbonic anhydrase-II by sulfamate and sulfamide groups: an investigation involving direct thermodynamic binding measurements, *J. Med. Chem.* 49 (2006) 3496–3500, <https://doi.org/10.1021/jm058279n>.
- [13] M. Vedadi, F.H. Niesen, A. Allali-Hassani, O.Y. Fedorov, P.J. Finerty, G.A. Wasney, R. Yeung, C. Arrowsmith, L.J. Ball, H. Berglund, R. Hui, B.D. Marsden, P. Nordlund, M. Sundstrom, J. Weigelt, A.M. Edwards, Chemical screening methods to identify ligands that promote protein stability, protein crystallization, and structure determination, *Proc. Natl. Acad. Sci. U. S. A.* 103 (2006) 15835–15840, <https://doi.org/10.1073/pnas.0605224103>.
- [14] D.P. Byrne, M. Vonderach, S. Ferries, P.J. Brownridge, C.E. Eyers, P.A. Eyers, cAMP-dependent protein kinase (PKA) complexes probed by complementary differential scanning fluorimetry and ion mobility-mass spectrometry, *Biochem. J.* 473 (2016) 3159–3175, <https://doi.org/10.1042/BCJ20160648>.
- [15] M. Sekiguchi, Y. Kobashigawa, H. Moriguchi, M. Kawasaki, M. Yuda, T. Teramura, F. Inagaki, High-throughput evaluation method for drug association with pregnane X receptor (PXR) using differential scanning fluorimetry, *J. Biomol. Screen* 18 (2013) 1084–1091, <https://doi.org/10.1177/1087057113491826>.
- [16] T.E. Carver, B. Bordeau, M.D. Cummings, E.C. Petrella, M.J. Pucci, L.E. Zawadzke, B.A. Dougherty, J.A. Tredup, J.W. Bryson, J. Yanchunas, M.L. Doyle, M.R. Witmer, M.I. Nelen, R.L. Desjarlais, E.P. Jaeger, H. Devine, E.D. Asel, B.A. Springer, R. Bone, F.R. Salemme, M.J. Todd, Decrypting the biochemical function of an essential gene from *Streptococcus pneumoniae* using ThermoFluor technology, *J. Biol. Chem.* 280 (2005) 11704–11712, <https://doi.org/10.1074/jbc.M413278200>.
- [17] M.W. Pantoliano, E.C. Petrella, J.D. Kwasnoski, V.S. Lobanov, J. Myslik, E. Graf, T. Carver, E. Asel, B.A. Springer, P. Lane, F.R. Salemme, High-density miniaturized thermal shift assays as a general strategy for drug discovery, *J. Biomol. Screen* 6 (2001) 429–440, <https://doi.org/10.1177/108705710100600609>.
- [18] M.W. Freyer, E.A. Lewis, Isothermal titration calorimetry: experimental design, data analysis, and probing macromolecule/ligand binding and kinetic interactions, *Methods Cell Biol.* 84 (2008) 79–113, [https://doi.org/10.1016/S0091-679X\(07\)84004-0](https://doi.org/10.1016/S0091-679X(07)84004-0).
- [19] J. Abbott, N. Livingston, S. Egri, E. Guth, C. Francklyn, Characterization of aminoacyl-tRNA synthetase stability and substrate interaction by differential scanning fluorimetry, *Methods* 2017 (2007) 64–71, <https://doi.org/10.1016/j.ymeth.2016.10.013>.
- [20] A. Neuenfeldt, B. Lorber, E. Ennifar, A. Gaudry, C. Sauter, M. Sissler, C. Florentz, Thermodynamic properties distinguish human mitochondrial aspartyl-tRNA synthetase from bacterial homolog with same 3D architecture, *Nucleic Acids Res.* 41 (2013) 2698–2708, <https://doi.org/10.1093/nar/gks1322>.
- [21] S.J. Hughes, J.A. Tanner, A.D. Hindley, A.D. Miller, I.R. Gould, Functional asymmetry in the lysyl-tRNA synthetase explored by molecular dynamics, free energy calculations and experiment, *BMC Struct. Biol.* 3 (2003) 5, <https://doi.org/10.1186/1472-6807-3-5>.
- [22] M. Vivoli, H.R. Novak, J.A. Littlechild, N.J. Harmer, Determination of protein-ligand interactions using differential scanning fluorimetry, *JoVE* (2014) 51809, <https://doi.org/10.3791/51809>.
- [23] D. Matulis, J.K. Kranz, F.R. Salemme, M.J. Todd, Thermodynamic stability of carbonic anhydrase: measurements of binding affinity and stoichiometry using ThermoFluor, *Biochemistry* 44 (2005) 5258–5266, <https://doi.org/10.1021/bi048135v>.
- [24] P. Cimperman, L. Baranauskienė, S. Jachimovičiūtė, J. Jachno, J. Torresan, V. Michailoviene, J. Matuliene, J. Sereikaite, V. Bumelis, D. Matulis, A quantitative model of thermal stabilization and destabilization of proteins by ligands, *Biophys. J.* 95 (2008) 3222–3231, <https://doi.org/10.1529/biophysj.108.134973>.
- [25] A. Zubriene, J. Matuliene, L. Baranauskienė, J. Jachno, J. Torresan, V. Michailoviene, P. Cimperman, D. Matulis, Measurement of nanomolar dissociation constants by titration calorimetry and thermal shift assay - radioligand binding to Hsp90 and ethoxzolamide binding to CAII, *Int. J. Mol. Sci.* 10 (2009) 2662–2680, <https://doi.org/10.3390/ijms10062662>.
- [26] N. Bai, H. Roder, A. Dickson, J. Karanickolas, Isothermal analysis of ThermoFluor data can readily provide quantitative binding affinities, *Sci. Rep.* 9 (2019) 2650, <https://doi.org/10.1038/s41598-018-37072-x>.
- [27] R. Mascarenhas, H.V. Le, K.D. Clevenger, H.J. Lehrner, D. Ringe, N.L. Kelleher, R.B. Silverman, D. Liu, Selective targeting by a mechanism-based inactivator against pyridoxal 5'-phosphate-dependent enzymes: mechanisms of inactivation and alternative turnover, *Biochemistry* 56 (2017) 4951–4961, <https://doi.org/10.1021/acs.biochem.7b00499>.
- [28] J.A. Bhayani, B.L. Hill, A. Sharma, A.A. Iglesias, K.W. Olsen, M.A. Ballicora, Mapping of a regulatory site of the *Escherichia coli* ADP-glucose pyrophosphorylase, *Front Mol Biosci* 6 (2019) 89, <https://doi.org/10.3389/fmolb.2019.00089>.
- [29] C.M. Figueroa, M.C. Esper, A. Bertolo, A.M. Demonte, M. Aleanzi, A.A. Iglesias, M.A. Ballicora, Understanding the allosteric trigger for the fructose-1,6-bisphosphate regulation of the ADP-glucose pyrophosphorylase from *Escherichia coli*, *Biochimie* 93 (2011) 1816–1823, <https://doi.org/10.1016/j.biochi.2011.06.029>.
- [30] C. Fusari, A.M. Demonte, C.M. Figueroa, M. Aleanzi, A.A. Iglesias, A colorimetric method for the assay of ADP-glucose pyrophosphorylase, *Anal. Biochem.* 352 (2006) 145–147, <https://doi.org/10.1016/j.ab.2006.01.024>.
- [31] B.L. Hill, R. Mascarenhas, H.P. Patel, M.D. Asencion Diez, R. Wu, A.A. Iglesias, D. Liu, M.A. Ballicora, Structural analysis reveals a pyruvate-binding activator site in the *Agrobacterium tumefaciens* ADP-glucose pyrophosphorylase, *J. Biol. Chem.* 294 (2019) 1338–1348, <https://doi.org/10.1074/jbc.RA118.004246>.
- [32] A. Savitzky, M.J.E. Golay, Smoothing and differentiation of data by simplified least squares procedures, *Anal. Chem.* 36 (1964) 1627–1639, <https://doi.org/>

- 10.1021/ac60214a047.
- [33] W.L. Butler, D.W. Hopkins, An analysis of fourth derivative spectra, *Photochem. Photobiol.* 12 (1970) 451–456, <https://doi.org/10.1111/j.1751-1097.1970.tb06077.x>.
- [34] R.S. Prajapati, S. Indu, R. Varadarajan, Identification and thermodynamic characterization of molten globule states of periplasmic binding proteins, *Biochemistry* 46 (2007) 10339–10352, <https://doi.org/10.1021/bi700577m>.
- [35] J.N. Weiss, The Hill equation revisited: uses and misuses, *Faseb. J.* 11 (1997) 835–841.
- [36] P.G. Telmer, B.H. Shilton, Insights into the conformational equilibria of maltose-binding protein by analysis of high affinity mutants, *J. Biol. Chem.* 278 (2003) 34555–34567, <https://doi.org/10.1074/jbc.M301004200>.
- [37] S. Szmelcman, M. Schwartz, T.J. Silhavy, W. Boos, Maltose transport in *Escherichia coli* K12. A comparison of transport kinetics in wild-type and lambda-resistant mutants as measured by fluorescence quenching, *Eur. J. Biochem.* 65 (1976) 13–19, <https://doi.org/10.1111/j.1432-1033.1976.tb10383.x>.
- [38] M.A. Ballicora, A.A. Iglesias, J. Preiss, ADP-glucose pyrophosphorylase, a regulatory enzyme for bacterial glycogen synthesis, *Microbiol. Mol. Biol. Rev.* 67 (2003) 213–225, table of contents. 10.1128/MMBR.67.2.213-225.2003.
- [39] T.H. Haugen, J. Preiss, Biosynthesis of bacterial glycogen. The nature of the binding of substrates and effectors to ADP-glucose synthase, *J. Biol. Chem.* 254 (1979) 127–136.
- [40] M. Paule, J. Preiss, Biosynthesis of bacterial glycogen: X. The kinetic mechanism of adenosine diphosphoglucose pyrophosphorylase from *Rhodospirillum rubrum*, *J. Biol. Chem.* 246 (1971) 4602–4609, <https://doi.org/10.1104/pp.109.149450>.
- [41] I. Segel, *Enzyme Kinetics: Behavior and Analysis of Rapid Equilibrium and Steady-State Enzyme Systems*, third ed., Wiley-Interscience, 1993.